ELSEVIER

Catalysis Communications 3 (2002) 51–60

CATALYSIS COMMUNICATIONS

www.elsevier.com/locate/catcom

A possible role for surface carbon during ethylene epoxidation over silver catalysts

Michael C.J. Bradford *, Digna X. Fuentes

CeraMem Corporation, 12 Clematis Avenue, Waltham, MA 02453, USA

Received 24 October 2001; received in revised form 10 January 2002; accepted 10 January 2002

Abstract

Evidence obtained during an investigation of ethylene epoxidation over unsupported silver powder and Ag–Cs/α-Al_2O_3 is used to present the hypothesis that some surface sites responsible for epoxidation may deactivate under some (but not all) experimental conditions as a consequence of surface carbon deposition and/or mild surface reconstruction facilitated by surface carbon. © 2002 Published by Elsevier Science B.V.

Keywords: Silver; Ethylene epoxidation; Reconstruction; Carbon

1. Introduction

Ethylene oxide, first produced by the reaction of ethylene chlorohydrin and potassium hydroxide in 1859, has been produced commercially via gas-phase ethylene epoxidation since ca. 1931 [1,2]. Currently, the worldwide production capacity of ethylene oxide exceeds 22 billion lb_m per annum [3], and according to the US Department of Energy, up to 29 trillion BTUs can be potentially saved through technology improvements related to ethylene oxide manufacture [4]. Therefore, there is a motivation to develop improved catalyst compositions that improve both catalyst performance and process energy efficiency.

The desired oxidation reaction is ethylene epoxidation to ethylene oxide:

$$C_2H_4 + \tfrac{1}{2}O_2 \rightarrow C_2H_4O \qquad \Delta H_{rxn} = -105 \text{ kJ/mol } C_2H_4 \tag{1}$$

However, complete combustion of the ethylene:

$$C_2H_4 + 3O_2 \rightarrow 2CO_2 + 2H_2O \qquad \Delta H_{rxn} = -1323 \text{ kJ/mol } C_2H_4 \tag{2}$$

as well as combustion of the ethylene oxide:

$$C_2H_4O + 2\tfrac{1}{2}O_2 \rightarrow 2CO_2 + 2H_2O \qquad \Delta H_{rxn} = -1218 \text{ kJ/mol } C_2H_4O \tag{3}$$

may also occur.

Historical catalyst development efforts have focused on modifications and promoters that inhibit combustion pathways and side reactions, such as the isomerization of ethylene oxide to acetaldehyde [5–16]. Catalysts employed in indus-

* Corresponding author.
E-mail address: mbradford@ceramem.com (M.C.J. Bradford).

1566-7367/02/$ - see front matter © 2002 Published by Elsevier Science B.V.
PII: S1566-7367(02)00049-3

try utilize silver supported by low surface area (< 3 m^2/g), low acidity supports, such as α-alumina or sintered silicon carbide. Trace amounts (ca. 0.1 wt%) of alkali promoters such as cesium are used to stabilize the "optimal" silver surface structure and the active surface oxygen species, as well as to adjust surface electron density and to neutralize acid sites on the support [17–19]. In addition, halide inhibitors such as chlorine are utilized via both catalyst modification and introduction of halocarbons such as 1,2-dichloroethane into the feed to promote ethylene oxide formation by either an ensemble or ligand effect, or both [19].

Several studies have indicated that both oxygen and chlorine can induce dynamic reconstruction of silver surfaces, and the epoxidation reaction may only occur on a small fraction of sites on the silver surface [19]. In addition, the dissolution of elemental carbon atoms into the silver sub-surface during the interaction of ethylene and oxygen on polycrystalline silver foil has been reported [20]. The phenomenon of adsorbate-induced restructuring of metal surfaces has been observed for a number of metal–adsorbate systems, such as carbon on Ni(1 0 0) and ethylene on Rh(1 1 1) [21]. Therefore, it is reasonable to question if surface carbon can form on, dissolve into, and/or reconstruct the silver surface during ethylene epoxidation, thereby resulting in an alteration of the catalyst performance.

Herein, evidence obtained during an investigation of ethylene epoxidation over unsupported silver powder and Ag–Cs/α-Al_2O_3 is used to present the hypothesis that some surface sites responsible for epoxidation may deactivate under some (but not all) experimental conditions as a consequence of surface carbon deposition and/or mild surface reconstruction facilitated by surface carbon.

2. Experimental

2.1. Catalyst preparation and characterization

Silver powder (Alfa Aesar, 99.99%) was used as-received without further modification. A Cs-promoted Ag/α-Al_2O_3 catalyst was prepared using a modified incipient wetness technique [22]. High-purity α-Al_2O_3 (99.99%, Ceralox HPA-1.0) was pre-calcined in flowing dry air (60 cm^3/h g_{cat}) for 2 h at 700 °C prior to use. Silver and cesium were introduced independently and sequentially to the calcined support material using aqueous solutions of $AgNO_3$ (Aldrich, 99.995%) and $CsNO_3$ (Aldrich, 99.99%), respectively. First, a nominal Ag/α-Al_2O_3 sample was prepared and calcined in flowing dry air for 2 h at 250 °C. Thereafter, cesium was added to the calcined Ag/α-Al_2O_3 catalyst to yield a nominal cesium loading of 0.20 wt%, and the Cs–Ag/α-Al_2O_3 catalyst was re-calcined in flowing dry air for 2 h at 250 °C.

Catalysts were characterized using direct current plasma emission spectroscopy to determine elemental composition. N_2 BET analysis was used to determine the surface area of the calcined α-Al_2O_3. Pulse N_2O chemisorption at 120 °C was used to estimate silver surface area and dispersion after cyclic pretreatment in hydrogen and oxygen [23–25]. Surface-weighted silver particle sizes were calculated from N_2O chemisorption data (d_{s,N_2O}) and silver dispersion (D) using $d_{s,N_2O}\,(\mathrm{nm}) = 1.34/D$ [24,25]. Powder X-ray diffraction (XRD) spectra were obtained using filtered Cu K_α radiation (Materials Characterization Laboratory at the Pennsylvania State University). In the case of "as-received" silver powder, the volume-weighted crystallite size (d_v) was estimated using the Scherrer equation, $d_v = 0.9\lambda/B\cos\theta$, with Warren's correction for instrumental line broadening, $B = (B_M^2 - B_I^2)^{1/2}$, where $\lambda = 1.5418$ Å for weighted Cu K_α radiation, B_M is the peak width at one-half maximum intensity, and B_I is the instrumental line broadening.

Spent catalyst samples were characterized ex situ via temperature programmed oxidation (TPO). After reaction, catalysts were cooled to room temperature in flowing argon, removed from the reactor, and subsequently transferred to a quartz tube packed with quartz wool. The quartz tube was placed in a horizontal tube furnace equipped with a carbon dioxide sensor at the effluent (Vaisala). Temperature-programmed oxidation of the catalysts in flowing dry air was thereafter performed at ca. 4 °C/min from 20 to 700 °C to quantify total carbon deposition (as either carbonaceous deposits or adsorbed CO_2).

2.2. Bench-scale apparatus for catalyst testing

High purity ethylene (99.5%), hydrogen (99.999%), argon (99.998%) and 9.0% oxygen in argon were introduced independently to the feed-gas manifold using mass flow controllers. The system used a tubular, fixed-bed reactor made of type 316 stainless steel. Electrical heating tape powered by a programmable temperature controller was used to control external reactor temperature, and up to three K-type thermocouples were placed inside the reactor to independently monitor the axial temperature gradient in the vicinity of the catalyst bed. The temperature of the reactor effluent line was typically maintained at 150–175 °C, and a back-pressure regulator was used to manually vary total reactor pressure between 100 and 1130 kPa. A manual gas-sampling port was located downstream of the back-pressure regulator for reactor effluent gas collection. Collected gas samples were injected into a gas chromatograph (SRI Model 8610A), separated with a HayeSep D column operating isothermally at 120 °C, and thereafter split for simultaneous analysis with flame ionization detector (FID) and thermal conductivity detector (TCD). The FID was used for methane, ethylene, ethylene oxide and acetaldehyde analyses, and the TCD was used for oxygen, carbon dioxide, ethylene and water analyses. Ethylene conversion and product formation rates were quantified from an overall carbon balance using TCD and FID response factors for methane, ethylene and carbon dioxide available in the literature [26], and an FID response factor for ethylene oxide determined using a gas calibration standard.

2.3. Catalyst testing

Typically, 0.6 g of ground and sieved catalyst [$0.125 \leqslant$ particle diameter (mm) $\leqslant 0.25$] was packed into the reactor between plugs of quartz wool, and thereafter purged overnight in flowing argon ($4500\ cm^3/h\ g_{cat}$). The following morning, the catalyst was subject to a pretreatment procedure similar to that suggested by Vannice and co-workers [24,25], involving multiple oxidation and reduction cycles at 170 °C. After pretreatment, the external reactor temperature was held at 240 °C and the catalyst was exposed to a mixture of ethylene and oxygen in argon ($O_2/C_2H_4/Ar = 8.1/9.1/82.8$, gas hourly space velocity = 5500 $cm^3/h\ g_{cat}$, weight hourly space velocity = 0.63 g $C_2H_4/h\ g_{cat}$). Catalyst activity and selectivity were fairly constant during the initial 6 h on stream; therefore, time-weighted average of these data are reported herein.

3. Results

3.1. Catalyst characterization

Catalysts were characterized via N_2 BET, N_2O chemisorption, and XRD; a summary of available data is provided in Table 1. The chemisorption uptake of atomic oxygen on the silver

Table 1
Surface areas, compositions, N_2O adsorption uptakes, and particle sizes for silver powder and Cs–Ag/α-Al_2O_3

Catalyst	S[a] (m^2/g)	Composition (wt%)[b]			O uptake[c] ($\mu mol/g_{cat}$)	Ag size (nm)[d]	
		Al	Ag	Cs		d_{s,N_2O}	d_v
Ag powder	0.42	–	99.99	–	7.80	1590	32
Cs–Ag/α-Al_2O_3	3.96 ± 0.06	46.4 ± 0.5	9.2 ± 0.7	0.2	12.9	64 ± 24	–

[a] The surface area of the Ag powder was estimated from the O uptake. The surface area for Cs–Ag/α-Al_2O_3 is that of the calcined support only and was obtained from N_2 BET.
[b] Elemental compositions (excluding Cs, for which the nominal value is listed) were determined via DCPES ($\pm 1\sigma_n$).
[c] Elemental O uptakes were determined via pulse N_2O decomposition at 120 °C.
[d] Surface-weighted particle sizes were primarily calculated from O uptakes after cyclic pretreatment in H_2/O_2 (d_{s,N_2O}) assuming an adsorption stoichiometry of $O/Ag_{surface} = 1$. Volume-weighted crystallite size (d_v) was calculated via XRD. See the discussion in the text for details.

Table 2
Catalyst performance for ethylene epoxidation (reaction conditions: $P = 100$ kPa; $T_{ext} = 240$ °C; $O_2/C_2H_4/Ar = 8.1/9.1/82.8$; GHSV = 5500 $cm^3/h\ g_{cat}$)

Catalyst	Conversion (%)[a]		Formation rate (μmol/s g_{cat})[a]			
	C_2H_4	O_2	CO_2	C_2H_4O	C_2H_4O selectivity[a,b] (%)	$TOF_{C_2H_4O}$ (s^{-1})[c]
Ag powder	21.0±1.2	40.6	1.29 ± 0.27	0.66 ± 0.13	50.7 ± 9.9	0.085 ± 0.017
Cs–Ag/α-Al_2O_3	3.1±0.4	4.0	0.10 ± 0.03	0.14 ± 0.01	75.1 ± 5.8	0.011 ± 0.001

[a] Conversion formation rates, and C_2H_4O selectivity are average values ($\pm 1\sigma_{n-1}$) observed over the duration of multiple experiments.
[b] Selectivity is defined as the molar rate of C_2H_4O formation normalized to the molar rate of C_2H_4 consumption.
[c] TOFs were estimated by normalizing specific activities (μmol/s g_{cat}) to O uptake during pulse N_2O chemisorption (μmol/g_{cat}) – from Table 1.

powder, as measured by pulse N_2O chemisorption after pretreatment in hydrogen and oxygen, corresponds to a silver surface area of 0.42 m^2/g [23]. The small volume-weighted crystallite size of 32 nm for the "as-received" silver powder indicates that these bulk silver particles are polycrystalline, and contain breaks in the long-term order, possibly due to grain boundaries or shear planes. The surface-weighted particle size of 64 ± 24 nm reported for silver in the Cs–Ag/α-Al_2O_3 catalyst was calculated as an average of two extremes by assuming either zero surface coverage of cesium on the silver surface (87 nm), or complete and exclusive adsorption of cesium on the silver surface (40 nm).

3.2. Catalyst performance

Catalyst performance for ethylene epoxidation was initially evaluated at 100 kPa after cyclic pretreatment in hydrogen and oxygen at 170 °C; a summary of these data is provided in Table 2. The measured ethylene oxide selectivity of ca. 51% over silver powder is quite similar to that of ca. 44% reported for unpromoted, alumina-supported, 56–100 nm silver particles [27]. The higher selectivity of ethylene oxide over the Cs–Ag/α-Al_2O_3 catalyst is expected due to a combination of cesium promotion and lower ethylene conversion.

In the evaluation of the kinetic data reported herein, established theoretical criteria were used for the preliminary assessment of the influence of mass and heat transfer; a brief review of these critera is available elsewhere [28]. Evaluation of the Weisz–Prater criterion demonstrated that the influence of intraparticle mass transfer on the observed global reaction rates was negligible. Application of the criterion of Anderson indicated that intraparticle heat transfer did not likely bias the kinetic results. In addition, the criterion of Mears was used to demonstrate that interphase heat transfer resistance was negligible in these experiments. Consequently, apparent turnover frequencies (TOFs) for ethylene oxide formation were estimated by normalizing specific activities for ethylene oxide formation (Table 2) to catalyst atomic oxygen uptakes at 120 °C (Table 1). The apparent TOF of 0.085 s^{-1} obtained for silver powder at 240 °C is larger than the apparent TOF of 0.011 s^{-1} obtained for the Cs–Ag/α-Al_2O_3 catalyst. Presumably, the relatively lower activity of this Cs–Ag/α-Al_2O_3 catalyst is a consequence of a relatively high coverage of cesium on the silver surface.

Additional catalyst performance data were obtained at elevated pressures up to 1130 kPa; a summary of the results obtained is provided in Table 3. In these experiments, the reaction was initially undertaken at a pressure of 100 kPa for several hours, followed by a slow but continuous increase in pressure until the desired final pressure was obtained. The total duration of this pressure transient was ca. 1 h. To facilitate comparison of these elevated pressure data with data obtained at atmospheric pressure (and shown in Table 2), data in Table 3 are normalized to corresponding data obtained at 100 kPa. In this regard, normalized values in Table 3 that are less than unity indicate a

Table 3
Influence of pressure on relative catalyst performance for ethylene epoxidation (reaction conditions (except pressure) are identical to those in Table 2)

Catalyst	P (kPa)	Rate ratio $(r_P/r_{P=100})$[a]		$C_P/C_{P=100}$[b]	$S_P/S_{P=100}$[c]
		CO_2	C_2H_4O		
Ag powder	100	1.00	1.00	1.00	1.00
	990	1.08	1.10	1.10	1.01
	1130	1.21	0.69	0.90	0.77
Cs–Ag/α-Al_2O_3	100	1.00	1.00	1.00	1.00
	1130	1.64	0.18	0.53	0.34

[a] Subscript P indicates the value of the parameter at the specified pressure in this table, and subscript $P = 100$ indicates the value of the parameter obtained at $P = 100$ kPa (data in Table 2).
[b] C is the ethylene conversion.
[c] S is the ethylene oxide molar selectivity, as defined in Table 2.

decrease in the parameter value at elevated pressure, and normalized values in Table 3 which are greater than unity indicate an increase in the parameter value.

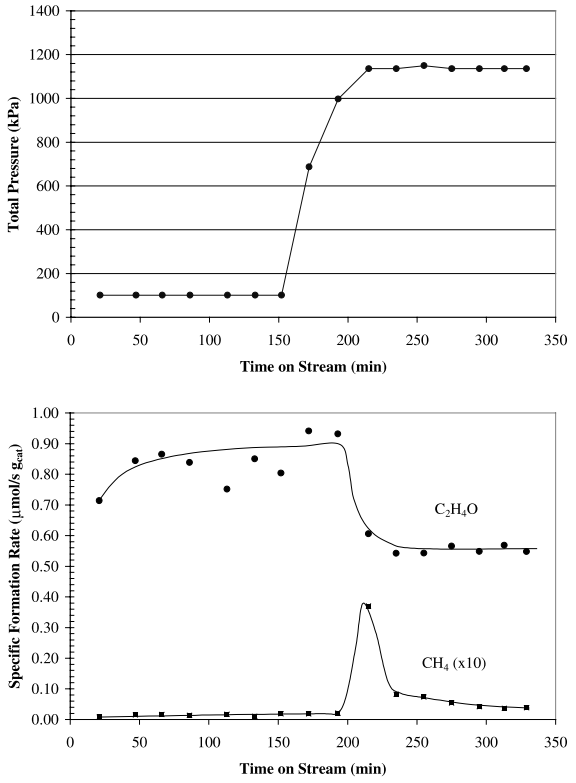

Fig. 1. Ethylene epoxidation over silver powder during a transient in total pressure from 100 to 1130 kPa. Reaction conditions: $T_{ext} = 240$ °C; $O_2/C_2H_4/Ar = 8.1/9.1/82.8$; GHSV = 5500 $cm^3/h\ g_{cat}$; WHSV = 0.63 g $C_2H_4/h\ g_{cat}$.

The increase of total system pressure from 100 to 990 kPa over silver powder resulted in a minor increase in the rates of ethylene conversion and carbon dioxide and ethylene oxide formation, although the selectivity to ethylene oxide was unchanged within experimental error. However, during experiments in which the pressure was raised from 100 to 1130 kPa, a marked transient in effluent methane concentration was observed at pressures exceeding 990 kPa (corresponding to an absolute ethylene partial pressure of 90 kPa), accompanied by a decrease in ethylene conversion and ethylene oxide production, as well as increased selectivity to carbon dioxide. An illustration of this phenomenon is provided in Fig. 1 (similar results were obtained for the Cs–Ag/α-Al_2O_3 catalyst during the 10–1130 kPa transient). It is unlikely that the observed change in the performance of silver powder during the pressure transient from 990 to 1130 kPa is a sole consequence of the kinetic acceleration of secondary reactions – such as ethylene oxide isomerization to acetaldehyde followed by rapid decomposition and combustion to yield methane, carbon dioxide and water – because the absolute rate of ethylene conversion also decreased markedly. The concomitant nature of methane formation and catalyst deactivation indicates that the phenomenon is associated with the catalyst surface. In addition, it is of interest to note that the sharp transient increase in methane production at $P > 990$ kPa is not maintained at steady state. This phenomenon may indicate a causal relationship, i.e., a particular type of surface

Table 4
Carbon accumulation on spent catalysts after ethylene epoxidation (reaction conditions are shown in Tables 2 and 3)

	Carbon removed (μmol CO_2/g_{cat})[a,b]		
Catalyst	100 kPa	990 kPa	1130 kPa
Ag powder	41	37	17
Cs–Ag/α-Al_2O_3	44	–	25

[a] Carbon removed was quantified via integration of $CO_2(t)$ evolution during TPO.
[b] The pressures indicated are the reactor pressures during ethylene epoxidation.

ensemble that is responsible for ethylene epoxidation (at $P < 990$ kPa) might have deactivated through the methane formation mechanism (at $990 < P(\text{kPa}) < 1130$).

3.3. Temperature programmed oxidation

Temperature programmed oxidation (TPO) of used catalysts was performed to quantify catalyst carbon content; a summary of these data is provided in Table 4. For these catalyst samples the total carbon deposition consistently decreased with increasing reaction pressure. In addition, the total carbon contents (Table 4) exceed atomic oxygen adsorption capacity, as determined separately via pulse N_2O decomposition (Table 1). For the Cs–Ag/α-Al_2O_3 catalyst, this observation is explicable as a consequence of carbon deposition and carbon dioxide chemisorption on the α-Al_2O_3 support, as well as the silver surface, during reaction. However, in the case of silver powder, the data indicate an apparent surface coverage for carbon ranging from ca. 2.2 (after reaction at 1130 kPa) to ca. 5.2 (after reaction at 100 kPa).

4. Discussion

During this investigation of ethylene epoxidation over bulk silver powder and a Cs–Ag/α-Al_2O_3 catalyst, two unexpected phenomena were observed. First, a continuous increase in reaction pressure above 990 kPa resulted in a decrease in ethylene conversion and ethylene oxide selectivity, as well as a transient increase in methane and carbon dioxide formation (Section 3.2). Second, the total amounts of carbon removed from the used catalysts after reaction exceed the adsorption capacities of each catalyst for atomic oxygen (Section 3.3). In this section, a hypothesis is presented to explain these observations; i.e., a potential exists for surface carbon and methane to form during ethylene epoxidation, and under certain conditions surface carbon might facilitate a subtle reconstruction of the silver surface. Thermodynamic calculations are presented to demonstrate that a potential exists for the formation of carbon and methane from mixtures of oxygen, ethylene and argon (Section 4.1). Bond order conservation–Morse potential (BOC–MP) calculations are presented to demonstrate that hydrogen abstraction by adsorbed oxygen is an energetically possible mechanism for the formation of surface carbon on the Ag(1 1 1) surface (Section 4.2). In addition, circumstantial evidence is presented to support the hypothesis that a potential exists for surface carbon to reconstruct the silver surface (Section 4.3).

4.1. Thermodynamic equilibrium

A series of thermodynamic calculations were performed (using HSC Chemistry v.4.1) to determine the potential for carbon and methane formation during ethylene epoxidation subject to the reaction conditions employed in this experimental study. Initial conditions were: $Ar/C_2H_4/O_2 = 828/91/81$, $T = 240$ °C and $P = 100$–1130 kPa. The free energy minimization calculations were limited by the restriction of possible reaction products to ethylene oxide, carbon monoxide, carbon dioxide, methane, water and graphite (chosen as a model representative carbon species). The calculation results are independent of total system pressure and indicate 100% conversion of both ethylene and oxygen at equilibrium, according to the following approximate reaction stoichiometry:

$$91C_2H_4 + 81O_2 \rightarrow 117.68C_{(s)} + 37.16CH_4 + 27.16CO_2 + 107.68H_2O \quad (4)$$

Although this production distribution was not observed experimentally during ethylene epoxida-

tion over supported silver catalysts due to intrinsic kinetic limitations, the thermodynamic results nevertheless indicate that a strong potential exists for both carbon and methane formation from ethylene in ethylene–oxygen mixtures.

4.2. Surface energetics

The thermodynamic equilibrium calculations in Section 4.1 indicate that there is a potential for carbon to form from ethylene–oxygen mixtures, provided that an energetically viable kinetic pathway exists for the transformation to occur. Presently, there is an absence of reports in the literature that discuss the energetics of carbon formation on silver surfaces during ethylene epoxidation. Therefore, in order to elucidate the existence of a possible kinetic pathway for surface carbon formation during ethylene epoxidation over supported silver, the BOC–MP method [29], which has been previously used to investigate the formation and reaction of allylic species [30] and the mechanism of methanol partial oxidation [31] on the Ag(1 1 1) surface, was employed.

A compilation of heats of adsorption for several surface species necessary for the estimation of activation energy barriers for relevant surface reactions on Ag(1 1 1) is provided in Table 5. It is worth noting that while the adsorption energies for O, H, OH and C species on Ag(1 1 1) were obtained directly from Shustorovich [29], Shustorovich employed a different heat of adsorption for C on Ag(1 1 1) in a subsequent work [30]. Regardless, this difference has no impact on the ultimate conclusions derived from these calculations. The heats of adsorption for CH_x and C_2H_x fragments were calculated using the formula for intermediate bonding of M_n–AB species [29]:

$$Q_{AB}(n) = \frac{1}{2}\left[\frac{Q_A^2}{\frac{Q_A}{n} + D_{AB}} + \frac{\left[Q_A\left(2-\frac{1}{n}\right)\right]^2}{Q_A\left(2-\frac{1}{n}\right) + D_{AB}}\right], \quad (5)$$

where $Q_{AB}(n)$ is the heat of adsorption of species AB at a surface site M_n with coordination number n, Q_A is the heat of adsorption of fragment A, and D_{AB} is the total bond energy of species AB. In the application of this equation it must be noted that values for n (limited to either 1, 2 or 3) were chosen based on the experimental observation that CH_x fragments on metal surfaces are preferentially located at adsorption sites that complete its tetravalency [32].

The activation energy barriers for some bond dissociation reactions (ΔE_{BD}) on the Ag(1 1 1) surface ($AB \rightarrow A + B$) were calculated directly from the data in Table 5 using the following equation [29]:

$$\Delta E_{BD} = Q_{AB} + \frac{1}{2}\left[D_{AB} + \frac{Q_A Q_B}{Q_A + Q_B} - Q_{AB} - Q_A - Q_B\right]. \quad (6)$$

Table 5
Bond energies (D_{AB}) and heats of adsorption (Q_{AB}) for monocoordinated M_n–AB species on Ag(1 1 1)

Species	D_{AB} (kcal/mol)	A	B	n	Q_{AB} (kcal/mol)	Reference
O	–	–	–	3	80	[29]
H	–	–	–	3	52	[29]
OH	102	O	H	–	55	[30]
C	–	–	–	3	120	[29]
CH	81	C	H	3	130	This work
CH_2	183	C	H_2	2	74	This work
CH_3	293	C	H_3	1	35	This work
C≡C	145	C	C	3	97	This work
HC≡C	259	C	CH	3	68	This work
H_2C=C	348	C	CH_2	3	55	This work
H_2C=CH	421	CH	CH_2	3	55	This work
H_3C–C	376	C	CH_3	3	52	This work
H_2C=CH_2	538	CH_2	CH_2	2	14	This work
CO	257	–	–	1	6.5	[31]
CO_2	384	–	–	1	3.2	[31]

Table 6
Activation energy barriers for some bond dissociation reactions (ΔE_{BD}) on the Ag(1 1 1) surface

Surface reaction	ΔE_{BD} (kcal/mol)
$H_2C{=}CH_2 \rightarrow H_2C{=}CH + H$	236
$H_2C{=}CH_2 \rightarrow CH_2 + CH_2$	220
$H_3C{-}C \rightarrow CH_3 + C$	150
$H_2C{=}C \rightarrow CH_2 + C$	127
$HC{\equiv}C \rightarrow CH + C$	70
$C{\equiv}C \rightarrow C + C$	31

A summary of activation energy barriers for several C_2H_x dissociation reactions is provided in Table 6. The results indicate that while the activation energy barriers for C_2H_x dissociation on Ag(1 1 1) decrease considerably with decreasing values of x, the only C_2H_x dissociation reaction (of those examined) that is likely not energetically prohibited is C≡C dissociation.

The activation energy barriers for hydrogen abstraction (ΔE_{HA}) from C_2H_x by adsorbed oxygen on the Ag(1 1 1) surface ($A + BC \rightarrow AB + C$) were calculated directly from the data in Table 5 using the following equation [29]:

$$\Delta E_{HA} = \frac{1}{2}\left[D + \frac{Q_{AB}Q_C}{Q_{AB}+Q_C} + Q_A + Q_{BC} - Q_{AB} - Q_C\right], \tag{7}$$

where $D = D_A + D_{BC} - D_{AB} - D_C \geqslant 0$. For reactions where $D < 0$, the activation energy for the reverse reaction (ΔE_r) was calculated from Eq. (7), and ΔE_{HA} was calculated directly from $\Delta E_{HA} = \Delta E_r - \Delta H_{rxn}$. A summary of activation energy barriers for several hydrogen abstraction reactions is provided in Table 7. The results indicate that the activation energy barriers for hydrogen abstraction by adsorbed oxygen are significantly lower than for C_2H_x dissociation ($\Delta E_{HA} \ll \Delta E_{BD}$), and are within a range that is, at least, energetically viable. Therefore, although surface carbon could conceivably form from surface reactions not represented by the simple reactions examined herein, it is concluded that hydrogen abstraction by surface oxygen from C_2H_x is a *possible* mechanism for surface carbon formation during ethylene epoxidation. This conclusion is consistent with recent "dipped-adcluster/Hartree–Fock/MP2" calculations which indicate

Table 7
Activation energy barriers for some hydrogen abstraction reactions (ΔE_{HA}) on the Ag(1 1 1) surface

Surface reaction	ΔE_{HA} (kcal/mol)
$H_2C{=}CH_2 + O \rightarrow H_2C{=}CH + OH$	13
$H_3C{-}C + O \rightarrow H_2C{=}C + OH$	14
$H_2C{=}C + O \rightarrow HC{\equiv}C + OH$	16
$HC{\equiv}C + O \rightarrow C{\equiv}C + OH$	22

that the energetically favorable reaction pathway for acetylene oxidation on silver surfaces is via hydrogen abstraction, resulting in the formation of surface acetylide and hydroxyl intermediates [33].

4.3. Surface carbon

A thermodynamic potential (Section 4.1) and a possible reaction mechanism (Section 4.2) exist for surface carbon formation during ethylene epoxidation over silver surfaces. Although BOC–MP derived activation energies for the surface reactions between atomic oxygen and carbon (0 kcal/mol) and between atomic oxygen and carbon monoxide (6 kcal/mol) indicate that carbon removal from the Ag(1 1 1) surface is facile, the accumulation of carbon on silver powder and Cs–Ag/α-Al_2O_3 catalysts was observed experimentally (Section 3.3). Therefore, inquiry about the nature and influence of surface carbon on silver surfaces is required.

In the case of silver powder, the observation of apparent carbon surface coverages exceeding one monolayer indicates the formation of large carbon deposits on the silver surface and/or subsurface carbon. During transient ethylene epoxidation experiments at elevated pressures, deactivation was not complete (Section 3.2), indicating that a significant fraction of the silver surface remained available to both oxygen and ethylene. The possible formation of multi-layer carbon deposits by either the Frank–van der Merwe or Stranski–Krastanov mechanisms is excluded from consideration because both mechanisms require the initial formation of a complete monolayer [21]. Therefore, the formation of carbon islands on the silver surface by a Volmer–Weber type of mechanism at particular sites on the silver surface through an overall reaction stoichiometry similar

to that described in Section 4.1 is possible. However, can these carbon species diffuse into the silver subsurface and/or induce a mild reconstruction of the silver surface? The phenomenon of adsorbate-induced restructuring of metal surfaces has been observed for a number of metal–adsorbate systems, such as carbon on Ni(1 0 0) and ethylene on Rh(1 1 1) [21]. Several studies have indicated that both oxygen and chlorine can induce dynamic reconstruction of silver surfaces [19], and the dissolution of elemental carbon atoms into the silver subsurface during the interaction of ethylene and oxygen on polycrystalline silver foil has been reported [20]. Therefore, it is reasonable to question if surface carbon can form on, diffuse into, and/or reconstruct a portion of the silver surface during ethylene epoxidation, thereby resulting in an alteration of the catalyst performance.

Proper quantitative analysis of this question involves a detailed analysis of surface reaction energetics and dynamics under relevant reaction conditions and is beyond the scope of the limited analysis herein. Nevertheless, a circumstantial argument is available to support the hypothesis that mild surface reconstruction by surface carbon is plausible. Specifically, the diatomic gas-phase bond dissociation energies [34] for Ag–O (53 ± 5 kcal/mol) and Ag–Cl (82 kcal/mol), as well as the heats of adsorption for atomic chlorine (53 kcal/mol – [30]) and oxygen (80 kcal/mol), exceed the diatomic bond dissociation energy for Ag–Ag (39 ± 2 kcal/mol), indicating that a thermodynamic potential exists for surface oxygen and chlorine to disrupt surface Ag–Ag bonds. The estimated heat of adsorption for carbon (120 kcal/mol) exceeds adsorption energies for chlorine and oxygen, as well as the diatomic gas-phase bond dissociation energy for Ag–Ag. Therefore, it might be inferred that adsorbed carbon and C_2H_x fragments (if present) can also disrupt surface Ag–Ag bonds, thereby resulting in a reconstruction of the silver surface during ethylene epoxidation.

If atomic carbon is present on the silver surface under conditions in which reconstruction (for example, by oxygen) is occurring, carbon atoms might diffuse to the subsurface in order to minimize the total energy of the surface layer by maximizing the extent of carbon–silver interactions. However, the calculated activation energy barrier for carbon diffusion within bulk silver is reportedly 73 kcal/mol [35]; therefore, bulk carbon diffusion would likely be restricted.

5. Summary

During a preliminary investigation of ethylene epoxidation over unsupported silver powder and Ag–Cs/α-Al_2O_3, a concomitant transient increase in methane formation and decreases in both ethylene conversion and ethylene oxide were observed during a transient in reaction pressure. Ex situ temperature programmed oxidation analysis of the used catalyst samples revealed that carbon surface coverages exceeded one monolayer. Thermodynamic calculations revealed that a strong potential exists for methane and carbon formation from ethylene–oxygen mixtures. Results from BOC–MP calculations indicate that surface carbon formation during ethylene epoxidation over Ag(1 1 1) is energetically viable through a mechanism involving hydride abstraction from surface C_2H_x species by adsorbed oxygen. In addition, simple energetic arguments indicate that perturbation of surface Ag–Ag bonds by surface carbon or C_2H_x species is possible. Therefore, it is proposed that some surface sites responsible for ethylene epoxidation over unsupported silver powder and Ag–Cs/α-Al_2O_3 may deactivate under some experimental conditions as a consequence of carbon deposition by a Volmer–Weber type of mechanism and/or mild surface reconstruction facilitated by surface and/or subsurface carbon species. Ultimately, however, additional work is necessary in order to either refute or support this hypothesis.

Acknowledgements

This work was funded by the National Science Foundation under SBIR Grant nos. DMI-9960419 and DMI-0109981. The authors thank CeraMem Corporation for permission to publish this work, and the manuscript reviewers for providing useful comments.

References

[1] B.J. Ozero, R. Landau, in: J.J. McKetta, W.A. Cunningham (Eds.), Encyclopedia of Chemical Processing and Design, Marcel Dekker, New York, 1984, pp. 274–318.
[2] J.P. Dever, K.F. George, W.C. Hoffman, H. Soo, fourth ed., Kirk-Othmer Encyclopedia of Chemical Technology, Vol. 9, Wiley, New York, 1994, pp. 915–959.
[3] G.H. Shahani, H.H. Gunardson, N.C. Easterbrook, Chem. Eng. Prog. 92 (11) (1996) 66.
[4] Energy and Environmental Profile of the US Chemical Industry. Office of Industrial Technologies, Department of Energy, May 2000.
[5] F.E. Cassidy, B.K. Hodnett, CATECH 2 (2) (1998) 173.
[6] J.E. Buffum, R.M. Kowaleski, W.H. Gerdes, US Patent #5,145,824 (1992).
[7] G. Boxhoorn, A.H. Klazinga, O.Velthuis, US Patent #4,728,634 (1988).
[8] S. Nagase, H. Tanabe, H. Imai, US Patent #5,395,812 (1995).
[9] N. Rizkalla, US Patent #5,736,483 (1998).
[10] R.A. Kemp, US Patent #5,545,603 (1996).
[11] S.F. Mitchell, D.M.A. Minahan, M.M. Bhasin, US Patent #5,051,395 (1991).
[12] W.L. Wernli, US Patent #4,087,385 (1978).
[13] S.D. Barnicki, J.R. Monnier, US Patent #6,011,163 (2000).
[14] S. Khoobiar, US Patent #4,169,099 (1979).
[15] W.H. Gerdes, C.M. Doddato, P.F. Malone, US Patent #5,100,859 (1992).
[16] B. Klopries, H. Metz, W. Dibowski, D. Kyewski, J. Pospiech, US Patent #5,668,077 (1997).
[17] S.N. Goncharova, E.A. Paukshtis, B.S. Bal'zhinimaev, Appl. Catal. A: Gen. 126 (1995) 67.
[18] V.I. Bukhtiyarov, I.P. Prosvirin, R.I. Kvon, S.N. Goncharova, B.S. Bal'shinimaev, J. Chem. Soc. Faraday Trans. 93 (1997) 2323.
[19] J.G. Serafin, A.C. Liu, S.R. Seyedmonir, J. Mol. Catal. A: Chem. 131 (1998) 157.
[20] V.I. Bukhtiyarov, A.I. Boronin, I.P. Prosvirin, V.I. Savchenko, J. Catal. 150 (1994) 268.
[21] G.A. Somorjai, Introduction to Surface Chemistry and Catalysis, Wiley/Interscience, New York, 1994.
[22] R.E. Kenson, M. Lapkin, J. Phys. Chem. 74 (1970) 1493.
[23] J.J.F. Scholten, J.A. Konvalinka, F.W. Beekman, J. Catal. 28 (1973) 209.
[24] S.R. Seyedmonir, D.E. Strohmayer, G.L. Geoffroy, M.A. Vannice, Adsorpt. Sci. Technol. 1 (1984) 253.
[25] M.V. Badani, M.A. Vannice, Appl. Catal. A: Gen. 204 (2000) 129.
[26] W.A. Dietz, J. Gas Chromatogr. (February) (1967) 68.
[27] V.I. Bukhtiyarov, I.P. Prosvirin, R.I. Kvon, S.N. Goncharova, B.S. Bal'zhinimaev, J. Chem. Soc. Faraday Trans. 93 (1997) 2323.
[28] R.J. Madon, M. Boudart, Ind. Eng. Chem. Fundam. 21 (1982) 438.
[29] E. Shustorovich, Adv. Catal. 37 (1990) 101.
[30] E. Shustorovich, Surf. Sci. 279 (1992) 355.
[31] B. Shen, X. Chen, K. Fan, J.-F. Deng, Surf. Sci. 408 (1998) 128.
[32] M.C.J. Bradford, M.A. Vannice, Catal. Rev. – Sci. Eng. 41 (1999) 1.
[33] Z.-M. Hu, H. Ito, S. Hara, H. Nakatsuji, J. Mol. Struct. (Theochem) 461–462 (1999) 29.
[34] CRC Handbook of Chemistry and Physics, 76th ed., CRC Press, Boca Raton, 1995.
[35] S. Dorfman, D. Fuks, M. Suery, J. Mater. Sci. 34 (1999) 77.